JOURNAL OF OPTOELECTRONICS AND ADVANCED MATERIALS Vol. 9, No. 8, August 2007, p. 2512 - 2515

# Influence of the substrate temperature on the optical and structural properties of magnetron sputtered ZnO thin films doped with Al and Er

D. DIMOVA-MALINOVSKA*, O. ANGELOV, H. NICHEV, M. KAMENOVA, J. C. PIVIN[a]
*Central Laboratory for Solar Energy and New Energy Sources, Bulgarian Academy of Sciences, 72 Tzarigradsko Chaussee Blvd., 1784 Sofia, Bulgaria*
[a] *CSNSM, CNRS-IN2P3, Batiment 108, 91405 Orsay Campus, France*

The influence of Al, and Er in ZnO thin films (ZnO:Al and ZnO:Er) deposited by magnetron sputtering at different substrate temperatures, Ts, on their optical and electrical properties was investigated. The optical band gaps, $E_{opt}$, of the films, from transmission and reflection spectra, ranged from 3.27 to 3.41 eV. The observed blue shift of $E_{opt}$ for the Al doped ZnO (ZnO:Al) was explained by the Burstein-Moss effect. The Urbach band tail width was also calculated. Incorporation of Al and Er resulted in a reduced and an increase resistivity, ρ, respectively, and an increase in the Urbach tail width in both cases. The ρ of ZnO:Al decreases with Ts, while for un-doped and Er doped ZnO films it increases. A discussion of the influence of $T_s$ and of Al and Er on the properties is presented.

(Received November 26, 2007; in revised form March 15, 2007; accepted April 2, 2007)

*Keywords*: Thin films, ZnO, Electrical properties, Structural properties, Optical properties

## 1. Introduction

Zinc oxide has gained much attention as a promising material for different applications in electronic and optoelectronic devices and sensors [1-4]. Investigation of the influence of doping with different elements on the properties of ZnO thin films is of a considerable importance for their possible applications for solar cells, displays and gas sensors.

In this work, a study of the influence of Al and Er, and of the substrate temperature, Ts, on the optical and electrical properties of ZnO thin films deposited by magnetron r.f. sputtering is reported.

## 2. Experimental

Thin films of ZnO were deposited by r.f. magnetron sputtering of ZnO or ZnO+1%$Al_2O_3$ ceramic targets in atmospheres of Ar (0.5 Pa) at $T_s$ values between 150 and 500 $^oC$. Discs of sintered ZnO and (ZnO(99at.%) + $Al_2O_3$ (1 at.%)), 100 mm in diameter, were used to deposit undoped (ZnO) and Al doped ZnO (ZnO:Al) films, respectively). The Al concentration in the films (measured by Rutherford Back Scattering, RBS) was about 2%. In the case of Er doping (ZnO:Er), Er chips were placed symmetrically on the ZnO target, in the zone of maximum erosion. The ratios of the ZnO target area to the Er chips area were 60:1 and 35:1 ($ZnO:Er_{60}$ and $ZnO:Er_{35}$ samples, respectively). The Er concentrations in the films (measured by Rutherford Back Scattering) were 0.20 and 0.40 at %, respectively. The vacuum chamber was evacuated to a residual gas pressure of 2. $10^{-4}$ Pa. Sputtering was carried out at an r.f. power of 180W. The thickness of the films was in the range 350 to 400 nm.

The X-ray diffraction (XRD) spectra were obtained using a DRON 3 spectrometer with CuKα radiation: λ $CuK\alpha_1$ = 1.540560 Å and λ $CuK\alpha_2$ = 1.544426 Å (intensity half that of λ $CuK\alpha_1$). The instrumental profile broadening was $0.08^0$ in 2Θ geometry. The resistivity of the films was calculated from the I-V characteristics, measured in the dark using a Keithley 6517 electrometer. The co-planar evaporated Al electrodes were verified to yield ohmic behaviour. Optical transmittance and reflection spectra were obtained in the range 300-1500 nm, using a CARY UV-VIS-NIR spectrophotometer.

## 3. Results and discussion

XRD analysis, obtained for 2Θ scans between $25^0$ and $75^0$, indicated that the deposited films were polycrystalline [5]. Reflections corresponding to the (002), (110), (102), (110), (103), (112) and (004) planes of wurtzite ZnO were observed (Fig. 1). The reflection corresponding to the (002) plane (a peak at about $2\Theta=34.40^0$) becomes more pronounced with increasing $T_s$, and the other reflections almost disappeared, which demonstrates the preferential (002) orientation of the grains in the films deposited at higher $T_s$. An improvement in the structural properties with increasing $T_s$ was observed for all sets of films. Only in the case of ZnO:Al was a deterioration of the crystalline structure observed with increasing $T_s$ from 150 to 275 $^oC$. However, further increase in $T_s$ resulted in an improvement of the structure of the ZnO:Al films. The (002) peaks showed a deviation from $34.44^0$, which is the value for ZnO powder (Table 1). A larger deviation was observed for ZnO films deposited at lower $T_s$ and those doped with Al and Er. These deviations indicate that the interplanar spacing increased relative to that of the ZnO

powder, which is probably due to factors such as lattice strain and interstitial defects [6]. The average grain size, D, in the films was calculated to an accuracy of about 10%, by applying the Scherrer equation to the Full Width at the Half Maximum (FWHM) of the (002) peaks [7]:

$$D = (K \lambda) / (\beta \cos \theta) \quad (1)$$

where $\beta$ is the value of FWHM, corrected for the instrumental function, K is the particle shape factor taken as 0.90. The FWHM of the peak corresponding to the (002) plane decreased with $T_s$ for ZnO and ZnO:Er films, which is an indication of an increased grain size. The incorporation of Al and Er resulted in smaller grain size in the films.

*Table 1. The values of the optical band gap, $E_g$, the Urbach energy, $E_o$, the 2Θ of (002) XRD peak, the value of its FWHM corrected for the instrumental function β, and the grain sizes for different series of ZnO films, deposited at different $T_s$.*

| Samples | $T_s$, $^0$C | $E_g$, eV | $E_0$, meV | $2\Theta$, deg. | $\beta$, deg. | Grain size, Å |
|---|---|---|---|---|---|---|
| ZnO | 150 | 3.33 | 63 | 34.30 | 0.52 | 160 |
| | 275 | 3.30 | 59 | 34.40 | 0.47 | 177 |
| | 500 | 3.27 | 60 | 34.40 | 0.33 | 252 |
| ZnO:Al | 150 | 3.36 | 100 | 34.20 | 0.62 | 136 |
| | 275 | 3.41 | 120 | 34.15 | 0.61 | 134 |
| | 500 | 3.33 | 91 | 34.27 | 0.62 | 134 |
| $ZnO:Er_{60}$ | 150 | 3.33 | 72 | 34.10 | 0.62 | 134 |
| | 275 | 3.34 | 70 | 34.30 | 0.62 | 134 |
| | 500 | 3.28 | 63 | 34.20 | 0.57 | 145 |

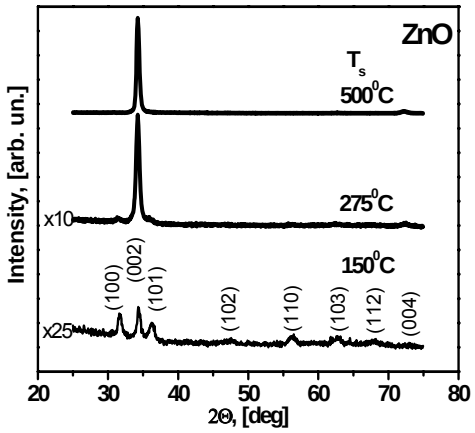


(a)

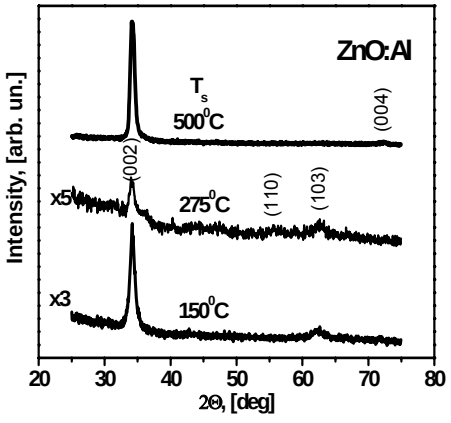


(b)

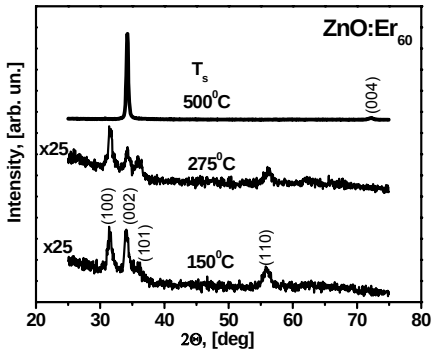


(c)

*Fig. 1. XRD patterns of the different series of ZnO films, deposited at different substrate temperatures, $T_s$: a) ZnO, b) ZnO:Al, c) $ZnO:Er_{60}$*

The transmission of all samples was about 92-93% for wavelengths higher than 600 nm, assuming a value of 100% for the transmission of the glass substrate. The absorption coefficient, α, was calculated as [8]:

$$\alpha(\lambda) = (1/d) \cdot \ln [ (1-R(\lambda))^2 / T(\lambda) ], \quad (2)$$

where $d$ is the film thickness, $T$ the transmittance and $R$ the reflectance.

The spectral dependence of α exhibited two regions: a power law one at high photon energies and an exponential one at lower energies. The formula for direct allowed transitions can be used to obtain the optical gap, $E_g$ [9]:

$$\alpha(h\nu) = A [(h\nu - E_g)^{1/2} / h\nu ] \quad (3)$$

The spectral dependences of the absorption coefficients for un-doped ZnO, Al doped ZnO (ZnO:Al) and Er doped ZnO (ZnO:Er) are shown in Fig. 2 a, b and c, respectively. The values for the optical gap and Urbach energy were calculated to an accuracy of 2%. The calculated energy gaps (3.27 – 3.41 eV) are typical for ZnO, and the values are given in Table 1. $E_g$ decreases with increasing $T_s$ for all sets of samples (except in the case of Al doping). The optical energy gap of the ZnO:Al thin films increases with increasing $T_s$ until 275 $^oC$, above which it decreases. The observed widening of the band gap in these films could be a result of the Burstein-Moss effect [10, 11]. The blue shift of $E_g$ in the Al doped ZnO films, as compared to un-doped ZnO films, could be due to an increase in the donor concentration, related to shallow Al donors. Incorporation of Er in the ZnO films does not influence $E_g$ significantly, compared to the value for undoped films.

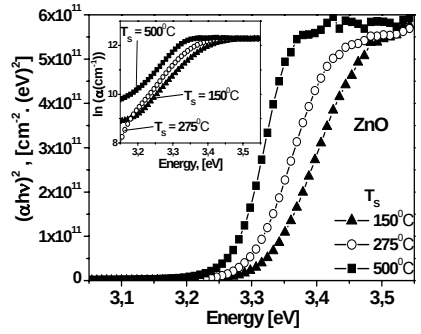


(a)

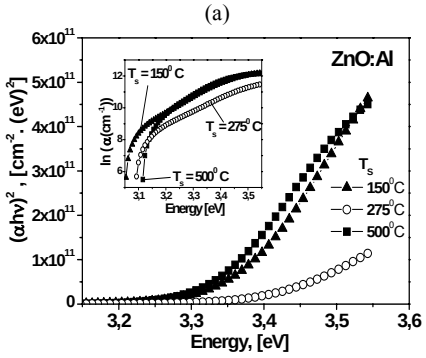


(b)

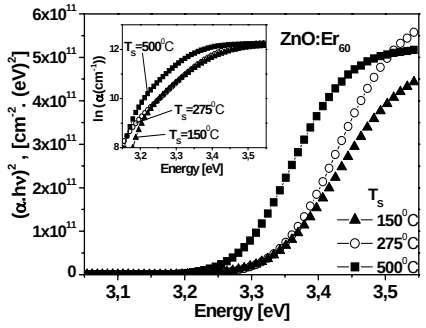


(c)

*Fig. 2. A plot of (α * hν)$^2$ against hν, for ZnO (a), ZnO:Al (b) and ZnO:Er$_{60}$ (c) thin films, deposited at different substrate temperatures, $T_s$. The insets show plots of ln α vs hν.*

In the lower energy range, where α varies exponentially with photon energy, it is possible to assume that the spectral dependence of the absorption edge follows the Urbach formula [12]:

$$(h\nu) = \alpha_0 \exp [ (h\nu - E_1)/E_0] \quad (4)$$

where $\alpha_0$ is the Urbach absorption at the edge ($E_1$), and $E_0$ is the Urbach energy width, which is believed to be a function of the structural disorder. The exponential dependence of the absorption on $h\nu$ in the Urbach region ($h\nu < E_g$) is due to the perturbation of the parabolic density of the states at the band edge – increasing structural disorder results in an increase in $E_0$ [12]. The energy dependences of $\alpha$ at lower photon energies are displayed in the insets of Fig. 2 a, b and c. The calculated Urbach energies are also given in these figures. It can be seen that doping with Al produces a significant increase in the Urbach band tail width, as compared to un-doped ZnO films – an indication of increasing structural disorder, which is confirmed by the XRD spectra. The incorporation of Er results in slight increases in $E_0$. It has to be noted that the deviations of the (002) peak position of the films under investigation, compared to the ZnO powder, which is proportional to the stress, correlate with the changes in Urbach energy. The stresses are higher in the doped ZnO films. The width of the Urbach tail decreases with increasing $T_s$ for all sets of samples, which could be related to an improvement in the structure of the ZnO films, as the XRD analyses show (see Table 1) [5,13].

Fig. 3 shows the resistivity, $\rho$, as a function of $T_s$ for all sets of samples. Here, the relationship between $\rho$ and the free carrier concentration, $n$, and mobility, $\mu$, has to be taken into consideration. The ρ decreases with increases in both $n$ and $\mu$. The carrier concentration is expected to decrease with increasing $T_s$, due to the oxidation of the Zn, Al or Er. The carrier mobility is expected to increase with increasing $T_s$, due to the improved orientation and grain size, and to a decrease in n [5, 12-14].

The resistivity of the un-doped ZnO films decreased slightly with increasing $T_s$ until about 275$^0$ C. This is probably related to an increase in $\mu$ due to the improved crystallinity of the films [13, 14], which is confirmed by XRD analysis - the grain size with (002) orientation increased from 160 to 252 Å with $T_s$ increasing from 150 to 275 $^oC$. Further increases in $T_s$ led to an increase in $\rho$ by 3 orders of magnitude. This could be related to the oxidation of interstitial Zn in the films, or to decreasing concentration of O vacancies at higher $T_s$, thus resulting in a decrease in n and an increase in ρ. It is probable that the effect of any possible increase in μ upon ρ is less pronounced than the changes in the stoichiometry of the films. Similar results are reported in [15].

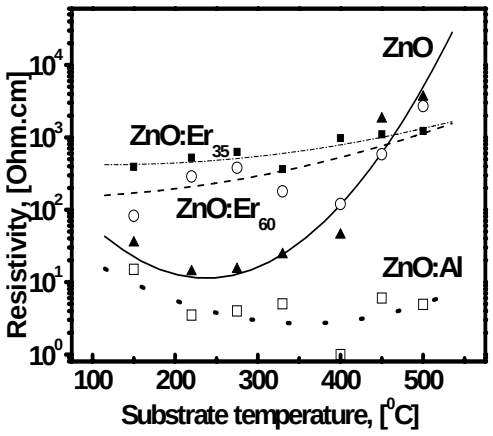


*Fig. 3. Dependence of the specific resistivity on the substrate temperature, $T_s$, of different ZnO, ZnO:Al, $ZnO:Er_{35}$ and $ZnO:Er_{60}$ films.*

The values of $\rho$ for the ZnO:Al films decreased with $T_s$ until about 400 $^oC$, and then increased slightly. Having in mind that the microstructure deteriorates with increasing $T_s$ up to 275 $^oC$ (as suggested by the increase in $E_0$, and from the XRD spectra), one can suppose that an increase in $n$ is the reason for the observed decrease in $\rho$. The size of the grains with (002) plane orientation was the smallest in ZnO:Al films (134-136 Å) and did not change with $T_s$. At higher $T_s$, it is possible that oxidation of the $Al^+$ and $Zn^+$ species will have an influence and the carrier concentration will drop, resulting in a slight increase in ρ.

The resistivity of the ZnO:Er thin films increased with the incorporation of Er at $T_s$ = 150 $^oC$, and also increased slightly with further increases in $T_s$. The higher $\rho$ values of these films compared to those of the un-doped ZnO films is possibly related to the partial oxidation of Er in the plasma during the co-sputtering - as a result $Er_2O_3$ would be present in the films. However, a higher Er concentration in the films ($ZnO:Er_{60}$) resulted in a slightly lower resistivity. This demonstrates that the presence of Er also probably contributes to the free carrier concentration.

## 4. Conclusions

Studies of the optical absorption and electrical resistivity of ZnO thin films, un-doped and doped with Al and Er, and their dependences upon the substrate temperature, have been performed. The spectral dependence of the absorption coefficient exhibited two regions: a power law and an exponential one. The value of the optical gap ranged from 3.27 to 3.41 eV for films deposited at different $T_s$. The optical gap increased with Al doping, which is explained by the Burstein-Moss effect. The Urbach tail width was calculated. Doping with Al and Er caused structural deterioration and a perturbation of the band structure – doping with Al led to higher structural disorder than for Er. The changes in the resistivity have been discussed in terms of the changes of the structural order of the films and possible oxidation of Zn, Al and Er with increasing substrate temperature.

**Acknowledgement**

This work is being performed with financial support from the Bulgarian National Scientific Fund – project UF 1505.

## References

[1] D. Dimova-Malinovska, N. Tzenov, N. Tzolov, L. Vassilev, J. Mater. Sci. Technol. **B52,** 59 (1998).
[2] Y. Cao, L. Miao, S. Tanemura, M. Tanemura, Y. Kuno, Y. Hayashi, Y. Mori, Jap. J. Appl. Phys. **45,** 1623 (2006).
[3] M. Aslam, V. Chaudhary, I. Mulla, S. Sainkar, B. Mandale, A. Belhekar, V. Vijayamohanan, Sensors and Actuator **75,** 162 (1999).
[4] N. Koshizaki, T Oyama, Sensors and Actuators **B66**, 119 (2000).
[5] D. Dimova-Malinovska, H. Nichev, O. Angelov, V. Grigorov, M. Kamenova, Superlatice and Microstructure (2007) in press.
[6] A. Kuroyanagi, J. Appl. Phys. **72**, 5492 (1989).
[7] B. E. Warren, X-ray Diffraction, Dover Publications Inc., New York (1990).
[8] J. Pankove, Optical Processes in Semiconductors, Prentice-Hall, Inc., New Jersey, (1971).
[9] D. Dragoman, M. Dragoman, Optical Characterization of Solids, Springer-Verlag, Heidelberg, (2002).
[10] F. Burstein, Phys. Rev. **93**, 632 (1954).
[11] T. S. Moss, Proc. Phys. Soc. **B67**, 775 (1954).
[12] M. Girtan, G. Folsher, Surf. Coat. Technol. **172,** 242 (2003).
[13] T. Minami, H. Sonohara, S. Takata, I. Fukuda, J. Vac. Sci. Technol. **A13,** 1053 (1995).
[14] D. Dimova-Malinovska, Thin Solid Films **36,** 179 (1976).
[15] A. P. Roth, D. F. Williams, J Appl. Phys. **52,** 6685 (1981).

*Corresponding author: doriana@phys.bas.bg